Passive reduction of large pressure variation for a high-speed express train in a narrow tunnel using an extra dummy tunnel duct [†]

Su-Hwan Yun,[1] Min-Ho Kwak,[1] Dong-Ho Lee,[1,*] Hyeok-Bin Kwon[2] and Tae-Hwan Ko[2]

[1]*Department of Mechanical & Aerospace Engineering, Seoul National University, Seoul, 151-742, Korea*
[2]*Korea Railroad Research Institute, Uiwang city, Kyonggi-Do 437-757, Korea*

Abstract

When a train travels through tunnel at a high speed, large pressure variations are produced on the train surface by pressure waves. In particular, when an express train travels through a narrow tunnel at a speed higher than that of a conventional train, more severe pressure variations can occur and cause passengers ear discomfort. This paper presents a very simple and effective reduction method of the large pressure variation for a narrow conventional tunnel. When a compression wave and an expansion wave are superposed, the pressure variation can be greatly reduced. Using this phenomenon, this study proposes the construction of a dummy tunnel duct which superposes the pressure waves and reduces the large pressure variation. Using the proposed method, the construction cost is much lower compared to other methods because the dummy tunnel duct can be constructed at the entrance or at the exit of an existing tunnel with a simple tunnel shape. To investigate the change in the maximum pressure difference and pressure variation ratio with the application of a dummy tunnel duct, full-scale tests and numerical analyses were conducted. The results showed that the maximum pressure changes and pressure variation ratio are significantly reduced by a short dummy tunnel duct. From these results, the dummy tunnel duct is expected to be a very economical and practical solution to passenger ear discomfort problems for express trains traveling through conventional narrow tunnels.

Keywords: Critical tunnel; Dummy tunnel duct; High-speed express train; Pressure wave Superposition; Pressure variation reduction

---

1. Introduction

A train entering a tunnel at a high speed generates compression and expansion waves that propagate through the tunnel at the speed of sound. As these pressure waves pass the train, large pressure changes are produced on the train surface. The surface pressure penetrates into the passenger car and causes ear discomfort to passengers. The large pressure fluctuations also place a sustained pressure load on the train surfaces, which can lead to cracks on these surfaces [1-2].

To reduce the pressure variation in a tunnel, numerous measures have been proposed and investigated. Some of the examples of these measures to alleviate severe pressure variation are listed below [3].

(1) Vehicle operational measures: reducing the tunnel entry and exit speed of a train

(2) Pressure sealing of rolling stock: making the vehicle sufficiently airtight

(3) Tunnel structural measures: construction of a tunnel with a larger cross-section or localized modification of a tunnel.

Though speed restrictions are feasible solutions, they are impractical considering the operating efficiency of the railway. Moreover, complete sealing is not only impossible considering the many systems on a passenger train, but it is also costly to adopt the special ventilation system needed in this case. The construction of a larger cross-sectional area requires an enormous cost. On the other hand, localized modifications of a tunnel, such as a flared or perforated entrance, are more practical and economical alternatives. Hagenah et al. measured and simulated the surface pressure of a train (SBB Re 460 and Cisalpino ETR 470) travelling through a tunnel with and without pressure relief shafts (A_{shaft}=12.25m^2). Their study, in a comparison of the pressure fluctuation between the tunnels, proved that pressure relief shafts give a higher degree of pressure comfort [4]. In addition, Kim et al. [5] and Bellenoue et al. [6] conducted scale-model tests and Yun et al. [7-8] conducted numerical analyses to verify the effects of a slit cover hood and a blind hood on tunnel-entrance for micro-pressure wave reduction. According to the results, both the slit cover hood and the blind hood reduced only the micro-pressure wave efficiently.
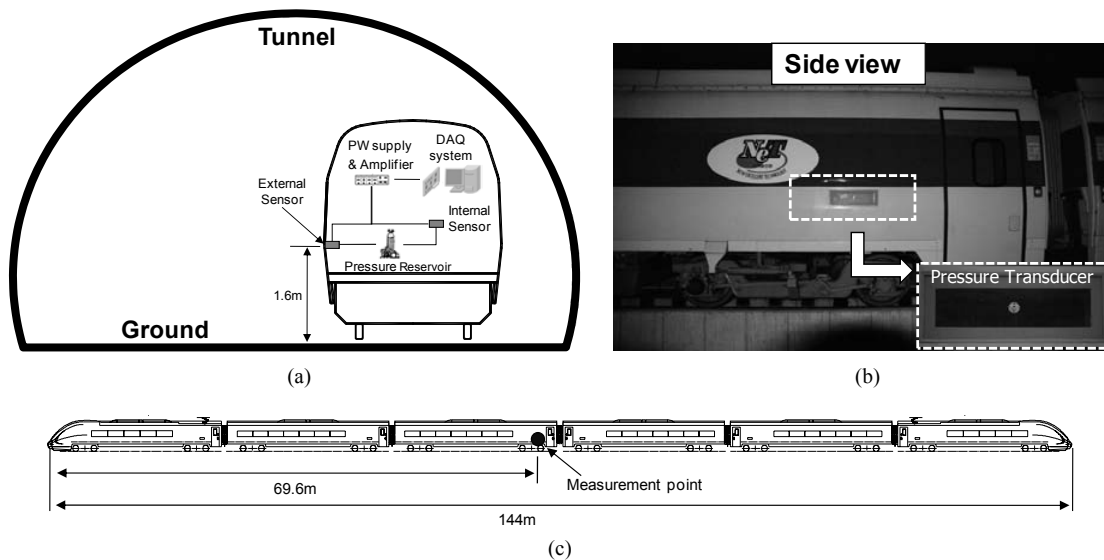

Fig. 1. Experimental set-up for the full-scale test: (a) Schematic view of the measurement system; (b) Pressure transducer mounted on the test train surface; (c) Location of pressure transducers on the middle car [10].

When a quasi high-speed express train travels existing conventional tunnels that are narrow and short, large pressure fluctuations can occur that can affect the comfort the passengers on the train. The objective of the present study is to reduce the large pressure variation in a tunnel when a train travels through the tunnel.

2. Experiment: field measurement

Full-scale tests were performed to obtain the surface pressure histories of a test train, while it traveled through a conventional tunnel at a high speed [9]. The test train was developed to increase the maximum commercial speed of a conventional train to 180km/h from 80~100km/h. The test train was 144m long and the cross-sectional area of the tunnel was $61m^2$ (blockage ratio: 0.161).

Fig. 1 shows the experimental apparatus for the full-scale test. A high sensitivity piezoresistive pressure transducer (ENDEVCO 8510B) and a Baraton differential manometer (MKS Type220) were used to measure the rapidly changing external and internal pressure of the train respectively, as it traveled through the tunnel. A pressure reservoir was used for the reference pressure supplier, as shown in Fig. 1(a). The external pressure transducer was mounted on the side surface of the train, as shown in Fig. 1(b). It was 69.6m from the nose-end and 1.6m from the ground, as shown in Fig. 1(a) and Fig. 1(c).

Fig. 2 shows the data acquisition process of the experimental system. The pressure transducer creates and transfers the differential pressure signals between the surface pressure and the reference pressure into the Amplifier module. The A/D converter with 16bits resolution then encodes the amplified output signals and transfers them to the data acquisition module. The digitalized data are sampled at a rate of 2kHz, filtered with a 100Hz low pass filter, and recorded in a storage device
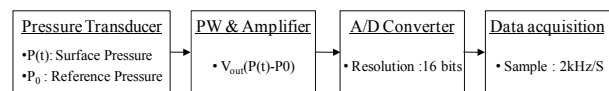

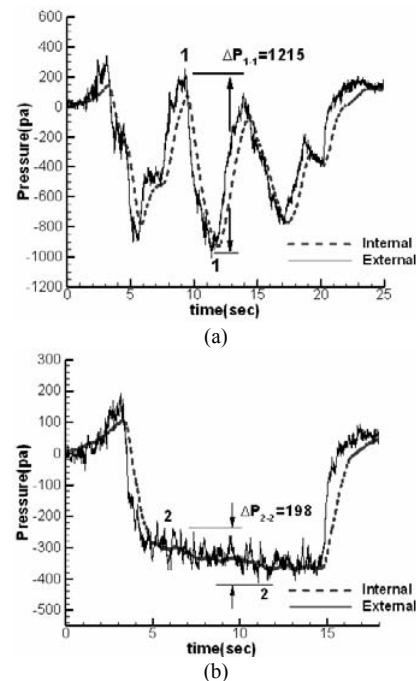Fig. 2. Data flow of the experimental apparatus.

Fig. 3. Measurement of surface pressure variation   (a) Large pressure variation (V_{tr}: 158km/h, L_{tu}:880m),   (b) pressure Variation reduction (V_{tr}: 147km/h, L_{tu}:570m) [9].

[10-12].

Fig. 3 shows internal and external (surface) pressure histories obtained while the test train traveled through conventional tunnels. Fig. 3(a) is a case in which the train passed through an
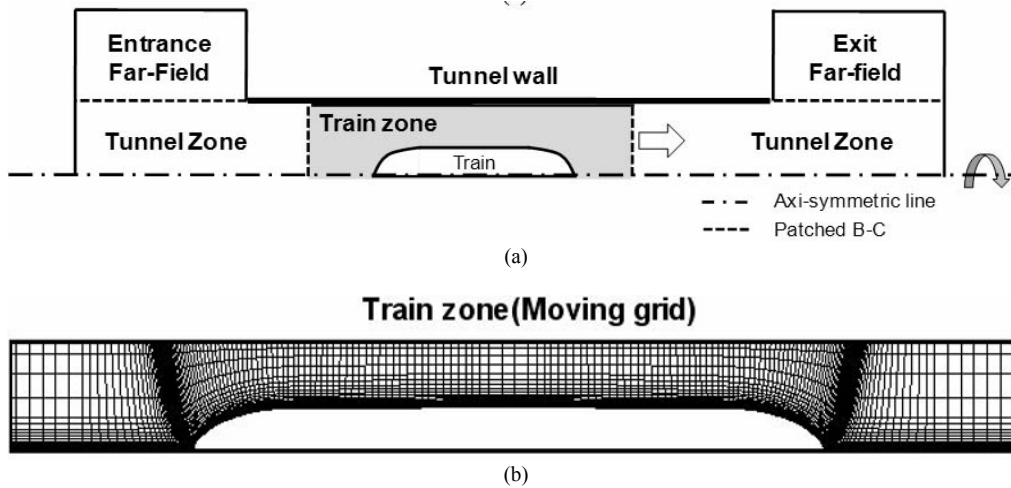
Fig. 4. (a) Composition of computational domains for an axi-symmetry numerical analysis, (b) Computational train model considered the cross-sectional area distribution of the test train [14].

880m long tunnel at 158km/h, and Fig. 3(b) is a case in which the train passed through a 570m long tunnel at 147km/h. A comparison of Fig. 3(a) and Fig. 3(b) shows that the trend curves of the pressure are very different from each other.

In Fig. 3(a), internal and external pressure fluctuations are very large. Hence, the maximum value of the pressure change is close to 1215pa (ΔP_{1-1}). On the other hand, in Fig. 3(b), large pressure fluctuations are not shown and the maximum value of the pressure variation is approximately 198Pa (ΔP_{2-2}) which is only 16.2% of that shown in Fig. 3 (a). In addition, these values remain nearly unchanged while the train travels through the tunnel.

The differences between Fig. 3(a) and Fig. 3(b) are simply the tunnel length (L_{tu}) and entry velocity (V_{tr}) of the test train. The results of a full-scale test suggest that large pressure variation on the train surface can be significantly reduced in an appropriate condition.
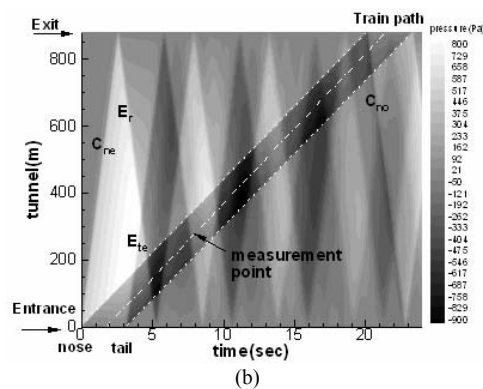
3. Numerical analysis

To investigate the pressure variation reduction of the full-scale test, numerical analyses were conducted. Although the flow fields generated by a train passing through a tunnel have three-dimensional and unsteady characteristics, the pressure wave propagation in a tunnel can be modeled as a one-dimensional compressible flow [13]. Moreover, three-dimensional numerical analyses require enormous computing resources and time. Therefore, in this study, Reynolds-averaged, unsteady, axi-symmetric compressible Navier-Stokes equation is used to save computing resource and time. The conservative form of the governing equation can be written as Eq. (1),

$$\partial_t \hat{Q} + \partial_\xi \hat{F} + \partial_\eta \hat{G} + H = \text{Re}^{-1}(\partial_\xi \hat{F}_v + \partial_\eta \hat{G}_v + H_v) \qquad (1)$$

where $\hat{Q}$ is the conservative variable vector, $\hat{F}$ and $\hat{G}$ are the flux vectors and H is the axi-symmetric source term.
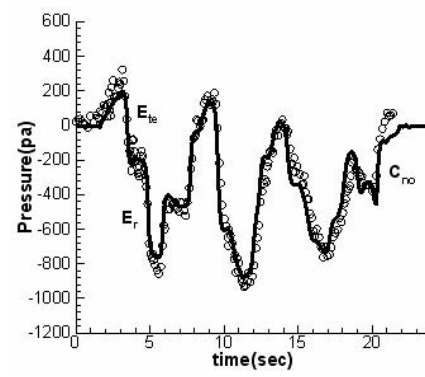
Fig. 5. (a) Comparison between measurements of full-scale test and computation; (b) pressure distribution of tunnel wall [9] (V_{tr}: 158km/h, L_{tu}:880m, —: numerical analysis, ○: full-scale test, E: Expansion wave, C: Compression wave, *ne*: nose-entry, *te*: tail-entry, *no*: nose-out, *r*:reflection).

Fig. 4(a) shows the composition of the computational zones for the axi-symmetric numerical analysis. The total computational domain consisted of four sub-domains (Entrance far, Exit far, Tunnel zone, Train zone). Among the sub-domains, Entrance far, Exit far and Tunnel zone sub-domains are stationary grids and only the Train zone sub-domain is a moving
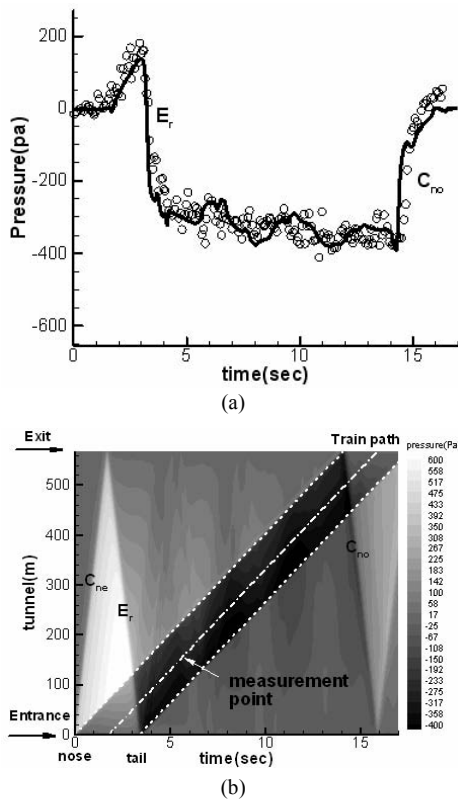
Fig. 6. Numerical results for the surface pressure variation reduction: (a) surface pressure history; (b) pressure distribution of tunnel wall (V_{tr}=147km/h, L_{tu}=570m, —: numerical analysis, ○: full-scale test, E: Expansion wave, C: Compression wave, ne: nose-entry, no: nose-out, r:reflection).

grid which is translated along the tunnel wall at the speed of the test train at every time step.

To consider the shape of the test train, a computational model in the Train zone was created with the same cross-sectional area distributions of the full-scale test train. The physical data of each domain can be exchanged through a patched boundary condition. The modified patched grid method was used principally to simulate the travelling motion of the train and to reduce the computation time in the Train zone [15].

3.1 Source of the surface pressure variation reduction

The numerical analysis results for a test train travelling through an 880m long tunnel at 158km/h are shown in Fig. 5. The surface pressure variations of the numerical results are compared with the full-scale test in Fig. 5(a). The solid line denotes the numerical results obtained at the location of the field measurement and the circles are the results of the full-scale test. The results of the numerical analysis are in good agreement with those of the full-scale test. Fig. 5(a) shows that the large pressure fluctuations were applied on the train surface, while it traveled through the tunnel.

Fig. 5(b) shows the pressure distribution on the tunnel wall. The dashed line and the dashed-dotted line indicate the trace
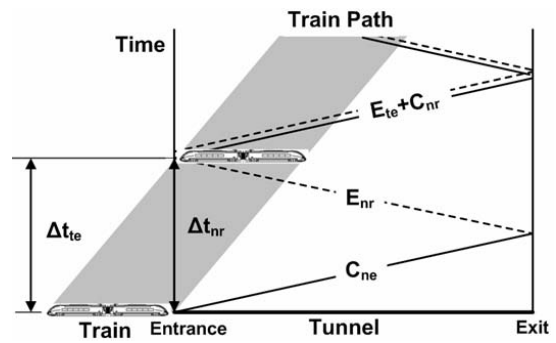

Fig. 7. Requirement for the superposition between pressure waves (— : compression wave, --- : expansion wave).

of the train and the measurement point of the surface pressure, respectively. Fig. 5(b) clearly shows that the pressure waves are generated (C_{ne}, E_{te}) at the entrance and are reflected (E_r) at the exit. Whenever the pressure waves pass the measurement point, the surface pressures largely and suddenly change, as shown in Fig. 5(a).

Fig. 6 shows the results of the numerical analysis when the test train traveled through a 570m long tunnel at 147km/h. The surface pressure change of the computational train during the passage is shown in Fig. 6(a). These results also show good agreement with the full-scale test.

In contrast to the large pressure variations shown in Fig. 5(a), however, small and gentle pressure changes are presented in Fig. 6(a). In Fig. 6(b), a tail-entry expansion wave is not shown when the tail of the train enters the tunnel. The pressure wave propagations also do not appear after the reflected expansion wave (E_r) arrives at the entrance. This situation arises due to the superposition between the compression wave and the expansion wave. Specifically, the compression wave converted from a reflected expansion wave (E_r) overlaps with the tail-entry expansion wave (E_{te}). This is a type of *destructive interference* of pressure waves.

3.2 Relationship between the train and the tunnel for the reduction of the pressure variation

When the *destructive interference* occurs, the shape of the resulting wave is determined by the sum of the separate amplitudes of each wave. Therefore, in order to reduce the pressure fluctuation via superposition, two pressure waves with the same amplitudes in the opposite direction are used. Moreover, they have to be completely overlapped [16, 17].

Fig. 7 shows the requirement for the superposition between a compression wave and an expansion wave. First, for the superposition, the tail-entry expansion wave (E_{te}) and the reflected compression wave (C_{nr}) have to be generated simultaneously. To ensure that this occurs, the time required ($\varDelta t_{nr}$) for the nose-entry compression wave (C_{ne}) to go and return to the tunnel has to be equal to that for the tail-entry expansion wave to be generated ($\varDelta t_{te}$)

Another requirement for the superposition is equal amplitudes of the pressure waves in the opposite direction. To com-
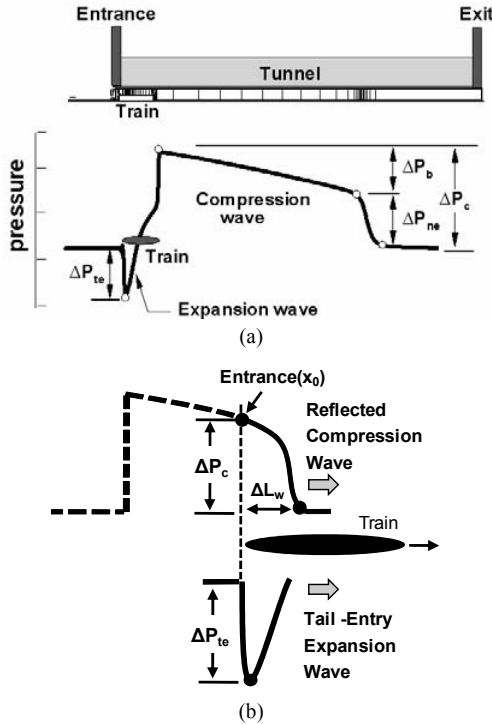
Fig. 8. (a) Compression and expansion wave form (*b*:body, *ne*:nose-entry, *te*:tail-entry); (b) arrangement of the pressure waves for the full destructive interference (ΔL_w: overlapping distance).

Fig. 9. (a) Change of pressure variation rate as a function of ΔL_w; (b) Surface pressure history at ΔL_w =0, 80, 220 (L_{tr}:144m, $\overline{V}_{tr}$: 180 km/h).

pare the amplitudes of the pressure waves, the pressure distribution along the tunnel wall is presented in Fig. 8(a) at the tail-entry moment.

In Fig. 8(a), both the compression wave propagating along the tunnel and the expansion wave generated by the tail-entry are shown simultaneously. The compression wave (ΔP_c) consists of two parts that cause the pressure increase. The first sudden pressure increase (ΔP_{ne}) is generated by the blockage effect between the tunnel and the train. The second gradual pressure increase (ΔP_b) is produced by a viscous effect. ΔP_c is continuously increased by the train body until the expansion wave (ΔP_{te}) is generated by the tail-entry of the train. It is well known that both ΔP_{ne} and ΔP_{te} mostly depend on the Mach number of the train and the blockage ratio [18, 19]. However, because ΔP_{te} generally has a larger amplitude than ΔP_{ne} [20], over propagation of the compression wave is required so that the positive amplitude (ΔP_c) increases at the same amplitude of the tail-entry expansion wave (ΔP_{te}). In this paper, the over propagation distance is termed *overlapping distance* (ΔL_w) and the tunnel, in which a pressure wave superposition can occur, is termed a 'critical tunnel'.

During the required time for the superposition, the compression wave propagates at the same distance of $2L_{cr} + \Delta L_w$, and the train travels the same distance as length of the train. Therefore, the required time can be defined using the train entry time and the total propagation time of the compression wave, as expressed by Eq. (2).
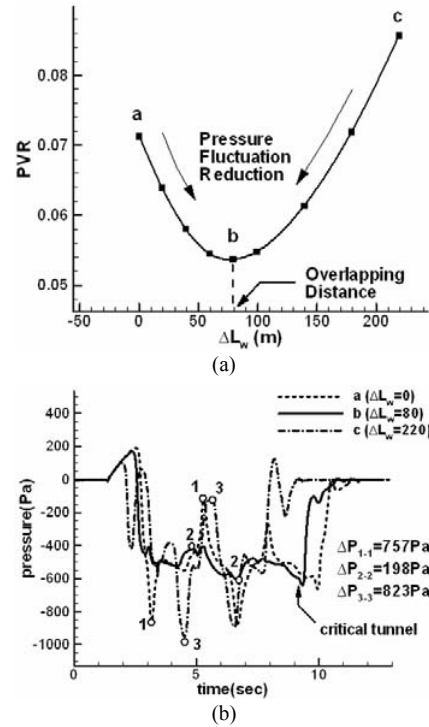
$$\Delta t_{te} = \frac{L_{tr}}{\overline{V}_{tr}} = \frac{2L_{cr} + \Delta L_w}{C(\overline{T})} = \Delta t_{nr} \qquad (2)$$

$\overline{V}_{tr}$	:	Mean entry velocity of train
L_{tr}	:	Length of train
L_{cr}	:	Length of critical tunnel
$C(\overline{T})$	:	Speed of sound
$\overline{T}$	:	Mean local temperature
ΔL_w	:	Overlapping distance

For an ideal superposition, the overlapping distance must be determined. To calculate the overlapping distance, the **p**ressure **v**ariation **r**ate (PVR) of the train surface is evaluated by means of numerical analysis. The **PVR** is calculated by Eq. (3). A high **PVR** indicates that a large pressure fluctuation occurs on the surface. On the other hand, a low value indicates that a small pressure fluctuation occurs.

$$PVR = \frac{1}{T} \int (P(t) - \overline{P})^2 \, dt \qquad (3)$$

T	:	Total travel time through the tunnel
P	:	Pressure of the train surface
$\overline{P}$	:	Mean value of the surface pressure

Fig. 9(a) shows the change in the **PVR** as a function of the overlapping distance. In Fig. 9(a), the **PVR** rapidly decreases as the overlapping distance increases from 0m to 80m. Around 80m, however, it shows a minimum value and no significant changes are presented. This indicates that a compression wave and an expansion wave are superposed by each other, which
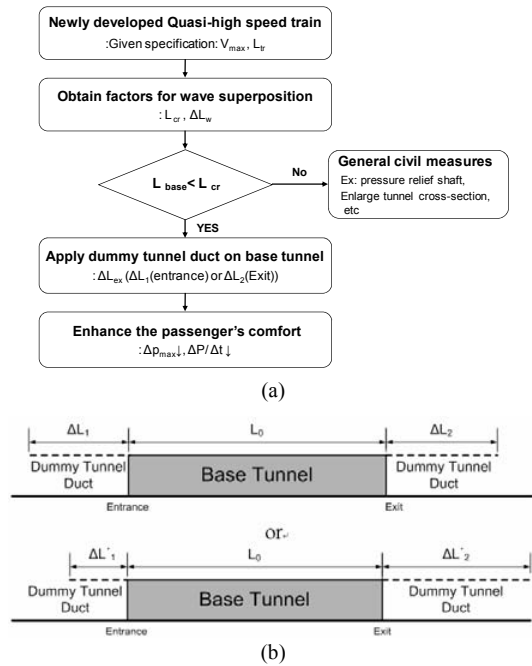
(a)

(b)

Fig. 10. (a) Application procedure of dummy tunnels for a quasi high-speed railway; (b) Construction adaptability of the dummy tunnel duct at tunnel portals ($\Delta L_1 + \Delta L_2 = \Delta L'_1 + L'_2 = \Delta L_{ex}$).

greatly reduces the large pressure fluctuation. Therefore, an overlapping distance with a minimum **PVR** value can be used for the overlapping distance of the ideal superposition. Beyond 100m, the **PVR** increases steeply again as the overlapping distance increases.

To prove the change of the surface pressure fluctuation for given overlapping distance (a (ΔL_w=0), b (ΔL_w=80) and c (ΔL_w=220)), the surface pressure histories are presented in Fig. 9(b). The pressure histories of a and c in Fig. 9(b) show a considerable amount of fluctuation. The maximum pressure difference of a and c is approximately 757Pa (ΔP_{1-1}) and 828Pa (ΔP_{3-3}), respectively. However, the pressure fluctuation of b is very small. Because the pressure waves are perfectly superposed with the ideal overlapping distance, the maximum pressure difference of b is only 198Pa (ΔP_{2-2}). Therefore, in this case, to create an ideal superposition between a compression wave and an expansion wave, an overlapping distance of 80m must be used.

4. Application of dummy tunnel duct for pressure variation reduction

The large pressure variation is naturally reduced in a critical tunnel. To change the existing base tunnel into a critical tunnel, a 'dummy tunnel duct' is proposed in this paper. It has a simple tunnel shape and can be constructed at the entrance or the exit of a base tunnel easily. Therefore, the required construction cost and modification time of a base tunnel can be reduced significantly.

Fig. 10(a) shows the application procedure of the dummy tunnel duct for an existing railway on which the newly devel-

Table 1. Specifications of the train and tunnel for the application of the dummy tunnel duct.

V_{max}	(km/h)	180
L_{tr}	(m)	200
L_{base}	(m)	550
L_w	(m)	80
L_{cr}	(m)	640

oped quasi high-speed train can travel. After the maximum operational speed (V_{max}) and the length (L_{tr}) of an advanced train are determined, the overlapping distance (ΔL_w) can be obtained. Then, the length of a critical tunnel (L_{cr}) is determined from Eq. (3). If the length of a base tunnel is shorter than that of the critical tunnel, the dummy tunnel duct (ΔL_{ex}) must be constructed at the portals (entrance (ΔL_1) or exit (ΔL_2)) of the base tunnel as much as the insufficient length compared to the critical tunnel length. Subsequently, although an advanced train travels through an existing tunnel at a higher speed, the pressure variation can be reduced and passenger comfort will be enhanced. In addition, the dummy tunnel duct has high adaptability for construction at the tunnel portals. A reduction of the large pressure variation can occur naturally, when the adapted dummy tunnel duct has the same total length (ΔL_{ex}). Therefore, in case it is impossible to construct at the entrance (ΔL_1) or the exit (ΔL_2), the length ($\Delta L'_1$, $\Delta L'_2$) of the each part of the dummy tunnel duct can be appropriately controlled, as shown in Fig. 10(b).

To investigate the effects of a critical tunnel using dummy tunnel ducts, numerical analyses were conducted for quasi high-speed express train travelling through an existing tunnel. The train length (L_{tr}) of a numerical model was 200m long and the maximum operating speed (V_{max}) was 180km/h. The length of the base tunnel (L_{base}) was 550m long, as listed in Table 1. If the over propagation distance (ΔL_w) is set to 80m, the length of the critical tunnel becomes 640m. Therefore, a 90m long dummy tunnel duct (ΔL_{ex}) is required for the critical tunnel. It is only 16.3% of the length of the base tunnel.

The critical tunnel length is defined by the objective maximum velocity and train length. Therefore, it is necessary to investigate the effects of other variables including the velocity, train length and blockage ratio. Figs. 11 and 12 show the effects of these variables while a train passes through the base tunnel without dummy tunnel duct and the base tunnel with dummy tunnel duct.

Fig. 11(a) shows maximum pressure variation (ΔP_{max}) as a function of the entry velocity. As the entry velocity increases from 160km/h to 180km/h, ΔP_{max} of the base tunnel ($\triangle$) gradually increases from 874Pa to 1023Pa. The maximum ΔP_{max} of the base tunnel is shown at the maximum speed (180km/h). However, in the case of a base tunnel with dummy tunnel duct ($\square$), ΔP_{max} rapidly decreases, in contrast to the base tunnel. It shows the minimum ΔP_{max} (403Pa) value at the maximum speed (180km/h). Therefore, the reduction ratio ($\blacksquare$) also increases from 11% (160km/h) to 60% (180km/h) as the train
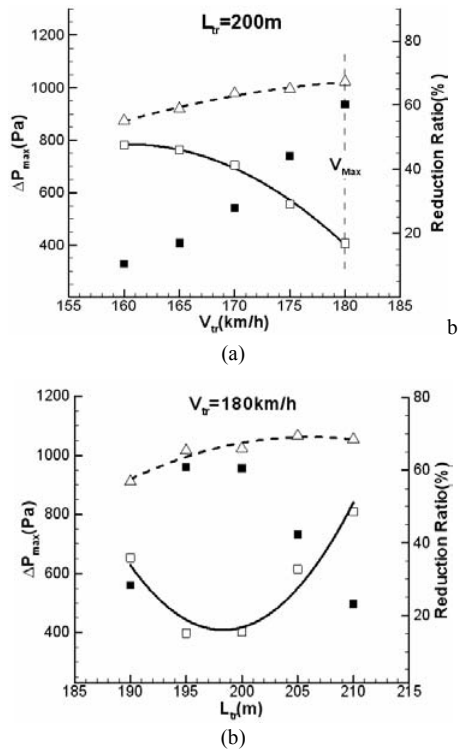
(a)

(b)

Fig. 11. Effects on the maximum pressure variation as a function of (a) the velocity and (b) the length of the train (Δ: base tunnel, □: base tunnel with dummy tunnel duct, ■:reduction ratio, blockage ratio: 0.161).
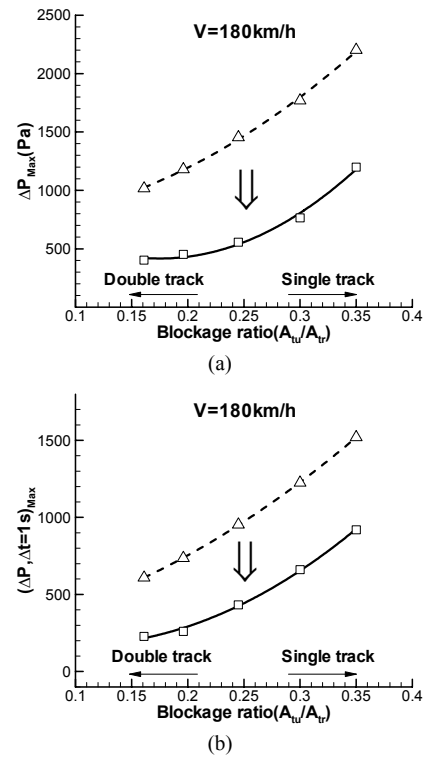

(a)

(b)

Fig. 12. Effects on Maximum pressure variation: (a) and Maximum pressure variation in time interval; (b) as a function of the blockage ratio (Δ: base tunnel, □: base tunnel with dummy tunnel duct).

velocity approaches the maximum speed.

Fig. 11(b) shows the change of ΔP_{max} as a function of the train length. ΔP_{max} of the base tunnel gradually increases from 911Pa to 1054Pa, as the length of the train increases from 190m to 210m. It is because of the viscous effect of the train body. In the case of base tunnel with dummy tunnel duct, ΔP_{max} changes greatly from 398Pa to 810Pa. Although the ΔP_{max} of the base tunnel with dummy tunnel duct changes more rapidly, this result shows that ΔP_{max} can be greatly reduced around a specific length (in this case from 195m to 200m). The maximum reduction ratio is, therefore, about 61% in that region.

Fig. 12(a) and (b) show the change of ΔP_{max} and $(\Delta P, \Delta t=1s)_{max}$ according to the blockage ratio (A_{tr}/A_{tu}) at a speed of 180km/h. $(\Delta P, \Delta t=1s)_{max}$ is the maximum surface pressure variation in time interval while the train travels through a tunnel. ΔP_{max} and $(\Delta P, \Delta t=1s)_{max}$ are usually used as criteria for travelling comfort or health risk of passengers in a vehicle [4]. Blockage ratio of a double-track tunnel and a single-track tunnel is approximately 0.16 and 0.32, respectively.

In Fig. 12(a), ΔP_{max} of the base tunnel is about 1021Pa at 0.16, and continuously increases with the increase of the blockage ratio. ΔP_{max} is about 2202Pa at 0.32. For the base tunnel connected by the dummy tunnel duct, however, ΔP_{max} becomes about 403Pa at 0.16. Therefore, ΔP_{max} is reduced by 60%. At 0.32, ΔP_{max} is about 1195Pa and ΔP_{max} is reduced by 45%.

In Fig. 12(b), $(\Delta P, \Delta t=1s)_{max}$ of base tunnel is about 609Pa

at 0.16 and about 1520Pa at 0.35. In case of base tunnel applied by dummy tunnel duct, $(\Delta P, \Delta t=1s)_{max}$ shows about 228Pa at 0.16 and 920Pa at 0.35 respectively. Therefore, the reduction ratio is about 62% and 39%. From Fig. 12(a) and (b), ΔP_{max} and $(\Delta P, \Delta t=1s)_{max}$ can be reduced significantly even in a single-track tunnel using the dummy tunnel duct.

5. Conclusion

This paper suggests a dummy tunnel duct to reduce the large and sudden pressure variation for an express train in a narrow conventional tunnel. For an evaluation of the effects of dummy tunnel duct, full-scale tests and numerical analyses were conducted. The conclusions are given below.

(1) The large and sudden pressure variation is greatly reduced when the reflected compression wave and the tail-entry expansion wave are perfectly superposed by each other at the entrance.

(2) For the superposition, the relationship among the variables (the velocity of the train, the length of the train, the length of the critical tunnel, the overlapping distance and the speed of sound) can be defined as $\dfrac{L_{tr}}{V_{tr}} = \dfrac{2L_{cr} + \Delta L_w}{C(\bar{T})}$.

(3) In the case of a 550m long base tunnel, only a 90m (16% of base tunnel) dummy tunnel duct is required for the superposition of pressure wave. As the express train velocity increases to the maximum operating speed (180km/h), ΔP_{Max} is rapidly decreased and reduced by 60% at the maximum

operating velocity, using dummy tunnel duct.

(4) In a double-track tunnel, ΔP_{max} and $(\Delta P, \Delta t=1s)_{max}$ can be reduced by 60% and 62%, respectively. In a narrow single-track tunnel, ΔP_{max} and $(\Delta P, \Delta t=1s)_{max}$ can be reduced by 45% and 39%.

When the length of an existing conventional tunnel is shorter than the critical tunnel, therefore, the construction of an optimum dummy tunnel duct is a very economical and practical solution to reduce the large pressure variation.

Acknowledgment

References

[1] R. S. Raghunathan, H.D. Kim, T. Setoguchi, Aerodynamics of high-speed railway train, *Progress in Aerospace Sciences*, 38 (2006) 469-514.

[2] S. Ravn and P. Reinke, Various aspects of aerodynamics and their implications on the design of the tunnels and underground stations of the magnetic levitation high-speed link in Munich (MAGLEV), *the 19th international conference on Magnetically Levitated systems and Linear Drives*, 2006.

[3] R. Gawthorpe, Pressure effects in railway tunnel, *Rail international scheinen der welt, INFRASTRUCURE*, 2000, 10-16.

[4] B. Hagenah and P. Reinke, Effectiveness of pressure relief shafts-full scale assessment, *12th International Symposium on Aerodynamics and Ventilation of Vehicle Tunnels*, 2006.

[5] D. H. Kim, D. H. Min and I. G. Oh, Experimental study of the aerodynamic countermeasures for reducing the micro-pressure waves and pressure fluctuations in high-speed train-tunnel interfaces, *World Congress on Railway Research*, Tokyo, Japan, October 19-23.

[6] M. Bellenoue, B. Auvity and T. Kageyama, Blind hood effects on the compression wave generated by a train entering a tunnel, *Experimental Thermal and Fluid Science*, 25 (2001) 397-407.

[7] S. H. Yun, B. Y. Kim, Y. C. Ku, D. H. Lee, H. B. Kwon and T. H. Ko, Numerical study of effects on micro-pressure wave reduction by a hood on a narrow tunnel, *Proceedings of the 2005 KSR Fall Conference*, 50-55 (in Korean).

[8] M. H. Kwak, Y. C. Ku, S. H. Yun, J. H. Rho and D. H. Lee, A study of tunnel entrance hood shape of High-Speed train with side running effect, *Proceedings of the 2009 KSR Spring Conference*, 483-488 (in Korean).

[9] A research project report 'Study on Aerodynamic Performance Evaluation of Korea Tilting train eXpress travelling a tunnel', Seoul National University, 2007 (in Korean).

[10] S. H. Yun, M. H. Kwak, D. H. Lee, H. B Kwon and T. H. Ko, Experimental Study of the Internal/external pressure variation of TTX travelling through a tunnel, *Journal of the Korean Society for Railway*, Vol.12, No.2, 2009, pp.309-314 (in Korean)

[11] T. Y. Kim, J. H. Hwang and D. H. Lee, An Experimental Study of Pressure Wave at Entering Tunnel for High-speed Train, *Proceedings of the 2001 KSAS Spring Conference*, 96-99 (in Korean)

[12] A research project report 'Development of Korea High-speed train (G7)', Seoul National University, 1996-1998 (in Korean).

[13] A. Yamamoto, Aerodynamics of Train and Tunnel, *Railway Technical Research Report*, No. 1230. Mar. 1983 (In Japanese).

[14] H. B. Kwon, A Study on the unsteady Compressible Flow Field Induced by a High-speed Train Passing through a Tunnel, Ph.D Thesis, Seoul National University, 2001.

[15] H. B. Kwon, K. H. Jang, Y. S. KIM, K. J. Yee, D. H. Lee, Nose shape optimization of High-speed train for Minimization of Tunnel Sonic Boom, *JSME international Journal Series C*, 44 (3) (2001) 890-899.

[16] I. G. Currie, Fundamental Mechanics of Fluids 3rd Ed, McGraw-Hill, 2007.

[17] A. R. Frey, Fundamentals of acoustics, John Wiley & Sons, 1999.

[18] W.-L. Mame and C. Tournier, A wave signature based method for the prediction of pressure transients in railway tunnels, *J. Wind Eng. Ind. Aerodyn*. 93 (2005) 521-531.

[19] M. S. Howe, Mach Number Dependence of the compression wave generated by a high-speed train entering a tunnel, *Journal of Sound and Vibration*, 212 (1) (1998) 23-36.

[20] H. D. Kim, S. H. Woo and D. H. Kim, Analytical Study on a Train-Induced Unsteady Pressure wave in High-Speed Railway Tunnel, *Proceedings of the KSME Spring Annual Meeting* 98'B,1998, 638-643 (in Korean).

Suhwan Yun is a Ph.D candidate at Seoul National University. He received his Bachelor's degree from Korea Aerospace University in 2003, and his Masters in 2005 from Seoul National University. He is a Ph.D candidate at Seoul National University. He is interested in Aerodynamics of high-speed train and aerodynamic shape optimization of the next generation ground vehicle.

Dongho Lee is a professor at Seoul National University. A member of the National Academy of Engineering of Korea. From 2007-2009 he was Director of the Institute of Advanced Aerospace Technology, Seoul National University. He is interested in Computational Fluid Dynamics, wind tunnel test and Multidisciplinary Design Optimization for large and complex systems.